Encapsulated Pd crystals on anatase supports: high precision determination of the titanate overlayer moiré structure

Yakun Gao,[a,†] Peiyu Chen,[a,*,†] and Martin R. Castell[a,*]

[a] Department of Materials, University of Oxford, Parks Road, Oxford OX1 3PH, United Kingdom

[*] Correspondence authors: peiyu.chen@materials.ox.ac.uk and martin.castell@materials.ox.ac.uk

[†] Y. G. and P. C. contributed equally to this work.

ABSTRACT

Palladium (Pd) crystal islands, with 100–200 nm wide (111) top facets, were grown in ultrahigh vacuum (UHV) on an anatase (001) film supported on a $SrTiO_3$(001) substrate. Annealing the crystals at > 600 ºC causes encapsulation by a TiO_x monolayer due to the strong metal–support interaction (SMSI). Scanning tunneling microscopy (STM) reveals that the TiO_x monolayer on the Pd(111) facets consists of two periodicities: one is a hexagonal $(4 \times 4)R1.5^{\circ}$ structure, and the other is a larger-scale periodicity consisting of a two-fold symmetric pattern of dark regions that can be described by a $(4\sqrt{39} \times 4\sqrt{61})R42.4^{\circ}$ superstructure. This double-periodicity structure requires a formation area of at least 100s of nm^2. An atomic model is developed that encompasses all features of the moiré superstructure.

1. Introduction

The strong metal–support interaction (SMSI) is a phenomenon of significant interest in materials systems where a noble metal catalyst is supported on a reducible oxide support such as oxides of Ti, Ce, and Nb. One of the popular materials systems is palladium (Pd) nanoparticles supported on TiO_2 substrates [1–5]. The SMSI occurs under reducing conditions and at elevated temperatures when a thin layer of TiO_x suboxide ($1 \leq x \leq 1.5$) migrates from the substrate onto the noble metal surface [1–10]. This thermodynamically-driven process occurs because the encapsulating oxide layer has a lower surface energy that the metal particle [11]. Encapsulation is of special interest in catalysis because it usually significantly reduces the catalytic activity of the noble metal, although on rare occasions it can enhance it. For example, encapsulated Pd nanoparticles demonstrate improved catalytic performance in the liquid-phase selective hydrogenation of phenylacetylene [4,5,8].

A number of studies have been published concerning the structure and stoichiometry of the encapsulating TiO_x suboxide layer and the reduced TiO_2 support. The presence is reported of Ti^{2+} [4,12], Ti^{3+} [2,13–15], or both species [1,11,16] in the encapsulating layers on Pd [1,2,4,11,12,15], Pt [14,16], and Au [13], by X-ray photoelectron spectroscopy (XPS) [1,4,11,12], electron paramagnetic resonance (EPR) [2], electron energy loss spectroscopy (EELS) [13,15], and density-functional theory (DFT) calculations [14,16]. The cross section of the TiO_x overlayer has also been directly observed in transmission electron microscopy (TEM), which is usually one or two monolayers in thickness [13,15,17,18].

Surface sensitive techniques such as scanning tunneling microscopy (STM) and low-energy electron diffraction (LEED) have been used to reveal the moiré superstructures formed by the TiO_x overlayer on (111) facets of noble metal nanocrystals, e.g., Pd [3,4,19] and Pt [1,6,7]. The Pt(111)–TiO_x structure was also studied by DFT calculations [7]. Encapsulated (001) facets of metal nanocrystals have not been directly observed but superstructures of TiO_x ultrathin films grown on Pd(001) [20,21] and Pt(001) [22,23] bulk substrates have been reported. The emerging consensus for TiO_x monolayer encapsulation of Pd(111) facets that have been annealed in ultrahigh vacuum (UHV) is that the Ti atoms are at the Pd interface and that the O atoms form the outer termination (Pd–Ti–O order) [2,4,15]. In addition, in many published STM studies of monolayers, Ti and O atoms show the same atomic periodicity. This points towards the same Ti and O atomic sublattices, indicating a 1:1 stoichiometric Ti:O ratio and hence a TiO monolayer [1,3,4,6,7,19].

Here, we report a study of Pd islands grown in UHV on an anatase thin film supported on a $SrTiO_3$(001) substrate. The Pd islands have (111) top and base facets and have typical widths of 100–200 nm. We observe that the Pd crystals treated at $\lesssim$ 600 ºC have smooth top facets [24] and those treated at $\gtrsim$ 600 ºC show moiré patterns, indicating that they have been encapsulated by a TiO_x layer [3]. Previously, we reported two types of six-fold symmetric moiré patterns between Pd(111) and TiO_x: the wagon wheel superstructure and the hexagonal superstructure [3]. In our previous paper, we reported on Pd crystals that were 10–20 nm in width, on which both superstructures were observed, and they could even coexist on the same crystal. In the work presented here, we find that small Pd crystals (< 10 nm in width) only exhibit the wagon wheel

superstructure, medium-sized Pd crystals (10–20 nm in width) can exhibit both, and large Pd crystals (100–200 nm in width) only form the hexagonal superstructure.

We believe that the reason why the moiré superstructure depends on the crystal size is that the lattice parameter of the epitaxial Pd crystals becomes closer to the relaxed bulk value as the crystals are increased in thickness. Small and thin crystals cannot relax in the same way as large islands due to the strong epitaxial interaction at the crystallographic interface with the substrate. In this paper, we focus on the large Pd islands, where our STM images reveal more detail of the hexagonal superstructure than previously published. We also present an atomic model that encompasses all features of this observed moiré pattern, based on geometrical construction and analytical modeling [3,25–27].

2. Experimental

The supporting $SrTiO_3$ crystals, which were doped with Nb at 0.5% by weight and epi-polished on the (001) surfaces, were supplied by PI-KEM, U.K. On the $SrTiO_3$(001) single crystal, we grew an anatase (1 × 4)-reconstructed TiO_2(001) film [28,29]. Pd was then deposited on the anatase substrate held at 300 ºC, from an *e*-beam evaporator using 99.95% pure Pd rods supplied by Goodfellow, U.K. The Pd islands were post-annealed in UHV at ≥ 600 °C for SMSI to occur. They were imaged by STM (JEOL JSTM 4500s model, base pressure 10^{-8} Pa). STM images were processed by *Gwyddion, WSxM* [30], *FabViewer* [31], and *Smart Align* [32,33].

3. Results and discussion

Figure 1(a) shows an STM image of small Pd crystals which were post-annealed at 600 °C for 1 h. They are typically < 10 nm in width and < 3 nm in height, with a wagon wheel superstructure on top. The anatase film supporting the crystals is characterized by ridges with a periodicity of 15.10 ± 0.15 Å, corresponding to a (1 × 4)-TiO_2(001) reconstruction [28]. Figure 1(b) shows a medium-sized encapsulated Pd crystal (width ~10.5 nm and height ~3.6 nm), showing the coexistence of the wagon wheel and the hexagonal superstructures, labeled as areas "W" and "H". The wagon wheel superstructure has a periodicity of 19.36 ± 0.63 Å and the hexagonal superstructure has a 11.01 ± 0.24 Å periodicity, in agreement with our previous report [3].

When a larger amount of Pd was deposited and post-annealed at 860 °C for 1.5 h, large Pd islands as shown in Fig. 1(c) were formed, which are typically 100–200 nm in width and > 20 nm in height. A hexagonal moiré pattern is observed on their top surface, which is due to the interaction between the Pd(111) lattice and the TiO_x overlayer. The higher annealing temperature of 860 °C for these large islands, compared with 600 °C for the smaller ones, was required to provide sufficient kinetic energy for the TiO_x layer to diffuse onto the much thicker crystals (> 20 nm) and form an equilibrium structure. The hexagonal moiré structure on large Pd islands is magnified in Fig. 1(e), in which the blue rhomboid unit cell exhibits a periodicity of 11.01 ± 0.24 Å. We also observe a larger-scale periodicity characterized by the regularly spaced darker regions. The corresponding unit cell is outlined by the yellow parallelogram, measured to be (6.88 ± 0.14) × (8.60 ± 0.07) nm^2 in size. The fast Fourier transform (FFT) of this image is shown in Fig. 1(d). The six-fold

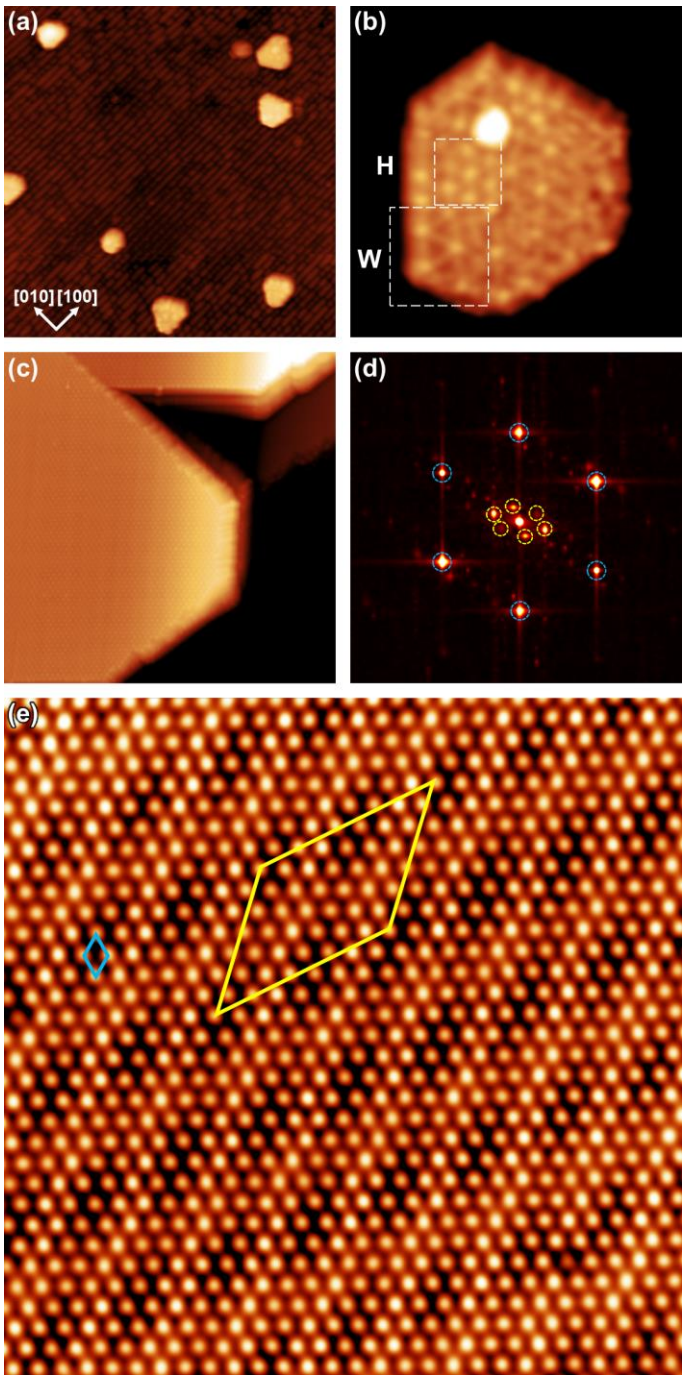

Fig. 1. TiO_x-encapsulated Pd islands: STM images of (a) small and (b) medium-sized Pd crystals supported on an anatase film (a: 76.2 × 76.2 nm^2, sample bias = 2.50 V, tunneling current = 0.83 nA; b: 14.5 × 14.5 nm^2, sample bias = 1.62 V, tunneling current = 0.25 nA). In (b) the wagon wheel structure is indicated by area "W" and the hexagonal structure by area "H". (c) STM image of large Pd islands (70.4 × 70.4 nm^2, sample bias = 1.97 V, tunneling current = 0.24 nA), (d) FFT and (e) STM image of the hexagonal moiré pattern formed between TiO_x and Pd(111) (30.8 × 30.8 nm^2, sample bias = 2.1 V, tunneling current = 0.17 nA). In (e), two types of unit cells are indicated by a blue rhombus and a yellow parallelogram, corresponding to the FFT spots circled in blue and yellow in (d).

symmetrical spots (circled in blue) correspond to the hexagonal moiré structure. Each of these spots has six satellites that are two-fold symmetrical (circled in yellow), corresponding to the periodicity described by the yellow parallelogram unit cell in real space.

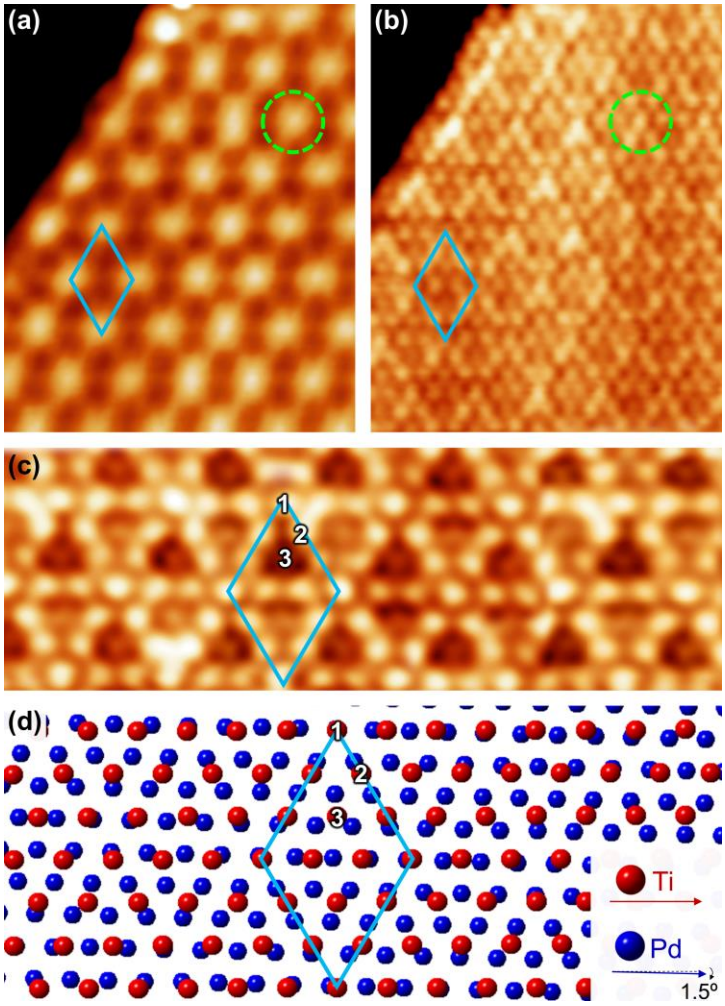

Fig. 2. (a) STM image of the hexagonal moiré pattern and (b) atomically resolved TiO_x layer of the same area (6.3 × 7.9 nm², a: sample bias = 0.45 V, tunneling current = 0.52 nA; b: sample bias = 0.66 V, tunneling current = 0.58 nA). The dashed green circle in (b) outlines seven Ti atoms comprising a moiré spot in (a). (c) Magnified STM image showing the Ti atoms (8.5 × 3.8 nm², sample bias = 0.48 V, tunneling current = 0.58 nA). (d) The atomic model in which a layer of Ti atoms (periodicity = 3.686 Å) is superimposed on a layer of Pd atoms (periodicity = 2.751 Å), with a rotational angle of 1.5° between them. In all panels, the (4 × 4) unit cell is outlined by a blue rhombus.

When the moiré pattern is imaged using a low bias and a high tunneling current, bright bridges

connecting the moiré dots are revealed, as shown in Fig. 2(a). Figure 2(b) is an atomically resolved image of the same area, where the bright spots are believed to be the Ti atoms in the TiO_x encapsulating layer. This is because under our imaging conditions the Ti atoms have a greater density of states than the O atoms and hence dominate the STM image [34]. It can be seen that each moiré dot is comprised of seven Ti atoms, as outlined by the dashed green circles. The atomic spacing of Ti atoms should therefore be a third of the moiré periodicity (11.01 ± 0.24 Å), and it is measured to be 3.66 ± 0.08 Å, consistent with previous literature [1,3,6]. Figure 2(c) shows a clearer STM image resolving the Ti atoms. The blue rhombi in all panels describe the same unit cell.

The recent scientific consensus is that the encapsulating TiO_x monolayer on Pd is O-terminated [2,4,15]. Therefore, to interpret the moiré pattern observed, we build an atomic model in which a Ti layer is superimposed on a Pd layer. By using the periodicity of Pd(111) = 2.751 Å and adopting the algebraic approach reported previously [3,25], we calculate that the periodicity in the Ti adlayer is 3.686 Å, and that the rotational angle between Pd(111) and the Ti adlayer is 1.5º. The Ti periodicity is consistent with our experimental measurement, 3.66 ± 0.08 Å. The atomic model in Fig. 2(d) is thus constructed using these parameters, where a six-fold symmetrical Ti layer (red atoms) is superimposed on a Pd(111) layer (blue atoms), with a rotational angle of 1.5º between them, as illustrated in the inset.

By inspecting the atomic model, we can term the moiré pattern a $(4 \times 4)R1.5^{\circ}$ superstructure with respect to the Pd(111) surface. In Fig. 2(c), some Ti atoms are brighter than others because of

topography. In general, three types of topographical positions are found, and an example of each is labeled. Type 1 is the brightest, when a Ti atom sits directly on top of a Pd atom. A type 2 Ti atom sits in a bridging site between two Pd atoms and its brightness is slightly lower. These Ti atoms are observed as bright lines connecting the moiré dots in Fig. 2(a). A type 3 Ti atom sits in a hollow site surrounded by three Pd atoms. It is topographically the lowest and hence the least bright in STM images.

In addition to the (4 × 4) periodicity, a larger pattern formed by dark regions is observed in the moiré pattern in Fig. 1(e). The two-fold symmetry suggests that the Ti atoms in the overlayer are not arranged in a perfect hexagonal way but are rather slightly compressed in one direction. Hence, we build the atomic model again in Fig. 3(a) and this time compress the Ti adlayer in a way depicted in Fig. 3(b), such that the angle α becomes slightly greater than 60º. We started by constructing atomic models with α varying from 60º to 70º with increments of 1º, and we blurred each model to resemble STM images. Only the model with α = 61º showed periodic dark regions. Thus, we narrowed down the range to $60º \leq \alpha \leq 61º$ with increments of 0.1º.

Some examples of the blurred atomic models ($60.0º \leq \alpha \leq 60.5º$) and their FFTs are shown in Fig. 3(c). Only the image with α = 60.3° shows an ordered dark-region pattern that reproduces the moiré structure in Fig. 1(e). The corresponding FFT also agrees with the experimental FFT in Fig. 1(d), where the main spots are six-fold symmetric (circled in blue), each surrounded by six satellites with two-fold symmetry (circled in yellow). The periodicity of the moiré dots is 11.06 Å, consistent with the STM measurement (11.01 ± 0.40 Å), as outlined by the blue rhombi unit cell in the α =

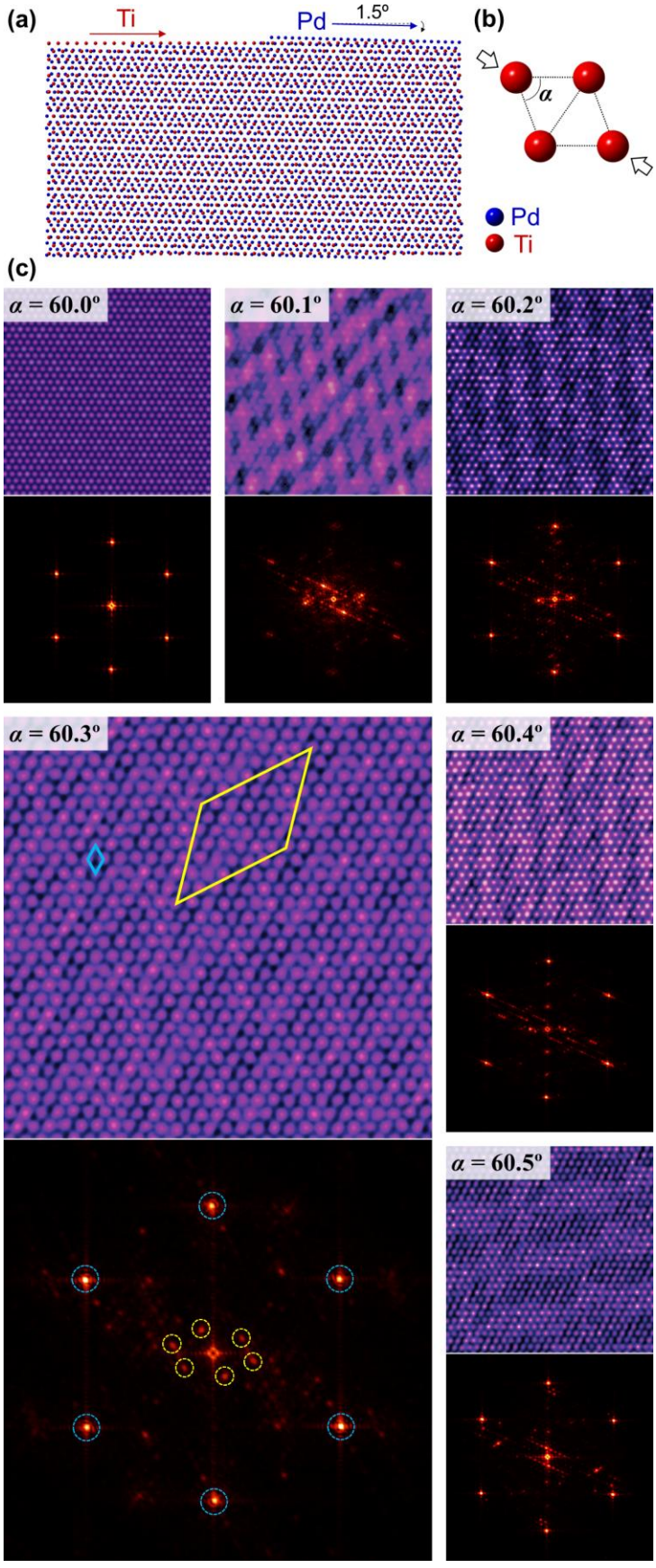

Fig. 3. Atomic models to simulate the moiré pattern. (a) A Ti layer (periodicity = 3.686 Å) is superimposed on a Pd layer (periodicity = 2.751 Å) with a rotational angle of 1.5º between them. The Ti layer is compressed in a way described by the unit cell in (b), with $\alpha > 60^{\circ}$. (c) Atomic models with different values of α are blurred to aid STM image interpretation. Below each atomic model is the corresponding FFT.

60.3º model. The dark-region pattern is characterized by the yellow parallelogram unit cell, which can be termed a $(4\sqrt{39} \times 4\sqrt{61})R42.4º$ superstructure with respect to Pd(111). It has a calculated size of 6.91 × 8.64 nm^2, consistent with our experimentally measured values, (6.88 ± 0.14) × (8.60 ± 0.07) nm^2.

4. Conclusions

In summary, we have grown large Pd islands (100–200 nm in width) in UHV on an anatase film supported on a $SrTiO_3$(001) substrate. After being annealed at 860 ºC for 1.5 h, the Pd is encapsulated by a TiO_x monolayer originating by diffusion from the substrate. The monolayer forms a hexagonal $(4 \times 4)R1.5º$ superstructure with the Pd(111) top facet, and the moiré pattern has a periodicity of 11.01 ± 0.24 Å. The moiré superstructure also shows periodic larger-scale dark regions with two-fold symmetry, which can be described by a $(4\sqrt{39} \times 4\sqrt{61})R42.4º$ superstructure, or a parallelogram unit cell of the size (6.88 ± 0.14) × (8.60 ± 0.07) nm^2. This double periodicity can only be observed on large Pd islands because of the relaxed nature of the top facet. A structural model is developed, in which a Ti layer is superimposed on a Pd layer, rotated by an angle of 1.5º and slightly compressed in one direction to open an angle of 60.3°, forming the observed hexagonal superstructure. We speculate that each of the moiré double periodicities might be associated with the creation of unusual electronic states, which could be investigated theoretically and experimentally.

Acknowledgements

This work was supported by EPSRC grant EP/K032518/1. The authors would also like to thank Chris Spencer (JEOL U.K.) for technical support and the China Scholarship Council (CSC) for financial support.

References

[1] R.A. Bennett, C.L. Pang, N. Perkins, R.D. Smith, P. Morrall, R.I. Kvon, M. Bowker, Surface Structures in the SMSI State; Pd on (1 × 2) Reconstructed TiO_2(110), J. Phys. Chem. B. 106 (2002) 4688–4696. doi:10.1021/jp0138328.

[2] Y. Li, Y. Fan, H. Yang, B. Xu, L. Feng, M. Yang, Y. Chen, Strong metal-support interaction and catalytic properties of anatase and rutile supported palladium catalyst Pd/TiO_2, Chem. Phys. Lett. 372 (2003) 160–165. doi:10.1016/S0009-2614(03)00383-X.

[3] F. Silly, M.R. Castell, Encapsulated Pd Nanocrystals Supported by Nanoline-Structured $SrTiO_3$(001), J. Phys. Chem. B. 109 (2005) 12316–12319. doi:10.1021/jp051358q.

[4] M. Bowker, P. Stone, P. Morrall, R. Smith, R. Bennett, N. Perkins, R. Kvon, C. Pang, E. Fourre, M. Hall, Model catalyst studies of the strong metal-support interaction: Surface structure identified by STM on Pd nanoparticles on TiO_2(110), J. Catal. 234 (2005) 172–181. doi:10.1016/j.jcat.2005.05.024.

[5] P. Weerachawanasak, P. Praserthdam, M. Arai, J. Panpranot, A comparative study of strong metal-support interaction and catalytic behavior of Pd catalysts supported on micron- and nano-sized TiO_2 in liquid-phase selective hydrogenation of phenylacetylene, J. Mol. Catal. A Chem. 279 (2008) 133–139. doi:10.1016/j.molcata.2007.10.006.

[6] O. Dulub, W. Hebenstreit, U. Diebold, Imaging cluster surfaces with atomic resolution: The strong metal-support interaction state of Pt supported on TiO_2(110), Phys. Rev. Lett. 84 (2000) 3646–3649. doi:10.1103/PhysRevLett.84.3646.

[7] D.R. Jennison, O. Dulub, W. Hebenstreit, U. Diebold, Structure of an ultrathin TiO_x film, formed by the strong metal support interaction (SMSI), on Pt nanocrystals on TiO_2(110), Surf. Sci. 492 (2001) L677–L687. doi:10.1016/S0039-6028(01)01460-1.

[8] Y. Li, B. Xu, Y. Fan, N. Feng, A. Qiu, J.M.J. He, H. Yang, Y. Chen, The effect of titania polymorph on the strong metal-support interaction of Pd/TiO_2 catalysts and their application in the liquid phase selective hydrogenation of long chain alkadienes, J. Mol. Catal. A Chem. 216 (2004) 107–114. doi:10.1016/j.molcata.2004.02.007.

[9] S.J. Tauster, S.C. Fung, R.L. Garten, Strong Metal-Support Interactions. Group 8 Noble Metals Supported on TiO_2, J. Am. Chem. Soc. 100 (1978) 170–175. doi:10.1021/ja00469a029.

[10] S.J. Tauster, Strong Metal-Support Interactions, Acc. Chem. Res. 20 (1987) 389–394. doi:10.1021/ar00143a001.

[11] Q. Fu, T. Wagner, S. Olliges, H.-D. Carstanjen, Metal-oxide interfacial reactions: Encapsulation of Pd on TiO_2 (110), J. Phys. Chem. B. 109 (2005) 944–951. doi:10.1021/jp046091u.

[12] M. Bowker, R. Sharpe, Pd deposition on TiO_2(110) and nanoparticle encapsulation, Catal. Struct. React. 1 (2015) 140–145. doi:10.1179/2055075815Y.0000000008.

[13] H. Tang, Y. Su, B. Zhang, A.F. Lee, M.A. Isaacs, K. Wilson, L. Li, Y. Ren, J. Huang, M. Haruta, B. Qiao, X. Liu, C. Jin, D. Su, J. Wang, T. Zhang, Classical strong metal–support interactions between gold nanoparticles and titanium dioxide, Sci. Adv. 3 (2017) e1700231. doi:10.1126/sciadv.1700231.

[14] G. Barcaro, S. Agnoli, F. Sedona, G.A. Rizzi, A. Fortunelli, G. Granozzi, Structure of reduced ultrathin TiO_x polar films on Pt(111), J. Phys. Chem. C. 113 (2009) 5721–5729. doi:10.1021/jp811020s.

[15] S. Zhang, P.N. Plessow, J.J. Willis, S. Dai, M. Xu, G.W. Graham, M. Cargnello, F. Abild-Pedersen, X. Pan, Dynamical observation and detailed description of catalysts under strong metal-support interaction, Nano Lett. 16 (2016) 4528–4534. doi:10.1021/acs.nanolett.6b01769.

[16] P. Finetti, F. Sedona, G.A. Rizzi, U. Mick, K. Schierbaum, G. Granozzi, Cation site environment in ultrathin TiO_x films grown on Pt(111) probed by X-ray absorption spectroscopy at the Ti 2p edge, Surf. Sci. 604 (2010) 366–371.

doi:10.1016/j.susc.2009.11.032.

[17] A.T. Bell, The Impact of Nanoscience on Heterogeneous Catalysis, Science. 299 (2003) 1688–1691. doi:10.1002/9783527679195.ch20.

[18] S. Liu, W. Xu, Y. Niu, B. Zhang, L. Zheng, W. Liu, L. Li, J. Wang, Ultrastable Au nanoparticles on titania through an encapsulation strategy under oxidative atmosphere, Nat. Commun. 10 (2019) 5790. doi:10.1038/s41467-019-13755-5.

[19] M. Bowker, E. Fourré, Direct interactions between metal nanoparticles and support: STM studies of Pd on TiO_2(110), Appl. Surf. Sci. 254 (2008) 4225–4229. doi:10.1016/j.apsusc.2008.01.014.

[20] M.H. Farstad, D. Ragazzon, H. Grönbeck, M.D. Strømsheim, C. Stavrakas, J. Gustafson, A. Sandell, A. Borg, TiO_x thin films grown on Pd(100) and Pd(111) by chemical vapor deposition, Surf. Sci. 649 (2016) 80–89. doi:10.1016/j.susc.2016.02.002.

[21] M.H. Farstad, D. Ragazzon, M.D. Strømsheim, J. Gustafson, A. Sandell, A. Borg, Oxidation and Reduction of TiO_x Thin Films on Pd(111) and Pd(100), J. Phys. Chem. B. 122 (2018) 688–694. doi:10.1021/acs.jpcb.7b06282.

[22] T. Matsumoto, M. Batzill, S. Hsieh, B.E. Koel, Fundamental studies of titanium oxide-Pt(100) interfaces I. Stable high temperature structures formed by annealing TiO_x films on Pt(100), Surf. Sci. 572 (2004) 127–145. doi:10.1016/j.susc.2004.08.006.

[23] T. Matsumoto, M. Batzill, S. Hsieh, B.E. Koel, Fundamental studies of titanium oxide-Pt(100) interfaces II. Influence of oxidation and reduction reactions on the surface structure of TiO_x films on Pt(100), Surf. Sci. 572 (2004) 146–161. doi:10.1016/j.susc.2004.08.005.

[24] P. Chen, Y. Gao, M.R. Castell, Experimental determination of the {111}/{001} surface energy ratio for Pd crystals Experimental determination of the {111}/{001} surface energy ratio for Pd crystals, Appl. Phys. Lett. 117 (2020) 101601. doi:10.1063/5.0022879.

[25] J. Hommrich, S. Hümann, K. Wandelt, Cadmium Underpotential Deposition on Cu(111) In Situ Scanning Tunneling Microscopy, Faraday Discuss. 121 (2002) 129–138. doi:10.1039/B200406M.

[26] M. Le Ster, T. Maerkl, P.J. Kowalczyk, S.A. Brown, Moiré patterns in van der Waals heterostructures, Phys. Rev. B. 99 (2019) 075422. doi:10.1103/PhysRevB.99.075422.

[27] M. Le Ster, T. Märkl, S.A. Brown, Moiré patterns: A simple analytical model, 2D Mater. 7

(2020) 011005. doi:10.1088/2053-1583/AB5470.

[28] F. Silly, M.R. Castell, Formation of Single-Domain Anatase TiO_2(001)-(1×4) Islands on $SrTiO_3$(001) after Thermal Annealing, Appl. Phys. Lett. 85 (2004) 3223–3225. doi:10.1063/1.1805177.

[29] M.S.J. Marshall, M.R. Castell, Shape Transitions of Epitaxial Islands During Strained Layer Growth: Anatase TiO_2(001) on $SrTiO_3$(001), Phys. Rev. Lett. 102 (2009) 146102. doi:10.1103/PhysRevLett.102.146102.

[30] I. Horcas, R. Fernández, J.M. Gómez-Rodríguez, J. Colchero, J. Gómez-Herrero, A.M. Baro, WSXM: A Software for Scanning Probe Microscopy and a Tool for Nanotechnology, Rev. Sci. Instrum. 78 (2007) 013705. doi:10.1063/1.2432410.

[31] F. Silly, A robust method for processing scanning probe microscopy images and determining nanoobject position and dimensions, J. Microsc. 236 (2009) 211–218. doi:10.1111/j.1365-2818.2009.03191.x.

[32] L. Jones, S. Wang, X. Hu, S. ur Rahman, M.R. Castell, Maximising the Resolving Power of the Scanning Tunneling Microscope, Adv. Struct. Chem. Imaging. 4 (2018) 7. doi:10.1186/s40679-018-0056-7.

[33] L. Jones, H. Yang, T.J. Pennycook, M.S.J. Marshall, S. Van Aert, N.D. Browning, M.R. Castell, P.D. Nellist, Smart Align—A New Tool for Robust Non-Rigid Registration of Scanning Microscope Data, Adv. Struct. Chem. Imaging. 1 (2015) 8. doi:10.1186/s40679-015-0008-4.

[34] U. Diebold, J.F. Anderson, K.-O. Ng, D. Vanderbilt, Evidence for the Tunneling Site on Transition-Metal Oxides: TiO_2 (110), Phys. Rev. Lett. 77 (1996) 1322–1325.